

Study of Non-Linear Optical Properties using Z-Scan

Mr. Shriman Keshri, R.No:1811150, 4th Year Int.M.Sc.,

School of Physical Sciences, National Institute of Science Education and Research,
HBNI, Jatni 752050, Odisha, India

08/05/2022

Abstract

In this experiment, we started learning nonlinear optics basics and their uses. Then we explored the Single Beam Z-Scan Technique and saw how Z-Scan traces for different materials could be obtained. We analyzed these traces using Python and saw how the Non-Linear Refractive Index and the Non-Linear Absorption Coefficient were calculated for toluene and acetone. We have also examined specific future directions in which we could take this experiment. We tried to make an optical transistor using the nonlinear refractive index property.

Contents

1	Objective	1
2	Overview	1
3	Theory	2
3.1	Nonlinear Optical Media	2
3.2	Nonlinear wave equation	2
3.3	Third-order Nonlinear Optics	2
3.3.1	Self-focusing and defocusing	3
4	Z-Scan Experimental setup	5
4.1	Apparatus used and their Working	5
4.2	Principle	6
4.3	Formulas to derive Nonlinear refraction and nonlinear absorption	7
5	Z-Scan Experiment	11
5.1	Toluene	11
5.1.1	Observation And Results	11
5.2	Acetone	13
5.2.1	Observation And Results	13
6	Conclusion	15
7	Improvement and New ideas on the Setup	15
7.1	Setup 1 and Explanation	15
7.2	Setup 2 and Explanation	15
7.3	Setup 3 and Explanation	17
7.4	Setup 4 and Explanation	17
8	Photos and Results	19
9	Advantages and Disadvantages of Z-Scan	20

10 Precautions and Sources of Error	20
11 References	20

1 Objective

- To study the basics of Non-Linear Optical Properties by using Z-scan Techniques.
- Taking measurements of transmitted power for open and closed aperture by translating the material in the z-direction.
- By fitting these data with the appropriate formulas, we will find the medium's nonlinear absorption coefficient and nonlinear refractive index for Acetone and Toulene.
- In the new idea section, try to make an Optical transistor, explain the things happening there, and suggest further improvement in the setup.

2 Overview

The non-linear optical properties of materials have found several applications in recent times, primarily in ultrafast optical switching and signal processing applications. In such cases, the relevant phenomena are Non-Linear Refraction (NLR) and Non-Linear Absorption (NLA). The Single Beam Z-Scan technique is one

of the principal techniques to explore these non-linear material characteristics owing to their simplicity and high sensitivity.

This technique can rapidly provide a measure of both NLR and NLA in solids as well as liquids (including solutions), yielding the sign as well as the magnitude of the non-linear refractive index and the non-linear absorption coefficient. This technique is based on the principles of spatial beam distortion. It makes use of the fact that a spatially transverse variation in LASER intensity induces non-linear optical changes in the material, giving rise to a lens-like effect, which in turn, affects the beam propagation. This leads to a self-focusing or defocusing effect (self-lensing effect). This, in turn, causes changes in the far-field diffraction pattern, that can be utilized to obtain the relevant non-linear optical properties of materials. "Single Beam," in the name, comes from the the fact that a single Gaussian laser beam in a tight focus geometry is used to induce the non-linear effects.

3 Theory

Nonlinear Optics is a branch of optics that deals with light behavior in nonlinear media(Polarization P relates non-linearly with electric field).

While considering nonlinear optical materials, two properties of interest are the material's nonlinear refractive index and its nonlinear absorption coefficients. Both change the intensity of light non-linearly when light passes through a medium.

The Z-Scan is based on the principle of spatial beam distortion used to measure the third-order optical nonlinearity and allows computing the contributions of nonlinear absorption and nonlinear refraction.

3.1 Nonlinear Optical Media

In a linear dielectric medium, there is a linear relation between Electric field and induced electric polarization.

$$\mathbf{P} = \epsilon_0 \chi \mathbf{E}$$

Where ϵ_0 is the electric permittivity of vacuum, and χ is the dielectric susceptibility of the medium. In a nonlinear dielectric medium, \mathbf{P} and \mathbf{E} are related non-linearly.

$$\mathbf{P}(\mathbf{E}) = \epsilon_0 \left(\chi^{(1)} \mathbf{E} + \chi^{(2)} \mathbf{E}\mathbf{E} + \chi^{(3)} \mathbf{E}\mathbf{E}\mathbf{E} + \dots \right)$$

Where $\chi^{(n)}$ are the higher-order susceptibilities that govern the nonlinear processes, when the intensity of the light is sufficiently high, only then these higher-order polarization terms will be significant.

3.2 Nonlinear wave equation

A wave equation for light propagation in a nonlinear medium can be derived from maxwell equations.

$$\nabla^2 \mathbf{E} - \frac{1}{c^2} \frac{\partial^2 \mathbf{E}}{\partial t^2} = \mu_0 \frac{\partial^2 \mathbf{P}}{\partial t^2}$$

We can write \mathbf{P} as sum of linear and nonlinear terms separately where \mathbf{P}_{NL} is $\mathbf{P}_{NL} = \chi^{(2)} \mathbf{E}\mathbf{E} + \chi^{(3)} \mathbf{E}\mathbf{E}\mathbf{E} + \dots$ equations, $n^2 = 1 + \chi$, $c = \frac{1}{n}$ and velocity of light in a Now, by using the equations, $n^2 = 1 + \chi$, $c = \frac{1}{n}$ and velocity of light in a medium of refractive index n , $v = \frac{c}{n}$, we can write wave equation in a nonlinear medium

$$\nabla^2 \mathbf{E} - \frac{1}{v^2} \frac{\partial^2 \mathbf{E}}{\partial t^2} = \mu_0 \frac{\partial^2 \mathbf{P}_{NL}}{\partial t^2}$$

This is the fundamental equation in the theory of nonlinear optics.

3.3 Third-order Nonlinear Optics

We generally work with centrosymmetric media (the properties of the medium which are not altered by the transformation $\mathbf{r} \rightarrow -\mathbf{r}$). Hence $\chi^{(2)}, \chi^{(4)}, \chi^{(6)}, \dots$ terms will vanishes. and hence third order term $\chi^{(3)}$ becomes more important. Equation (2.2) will become

$$\mathbf{P}(\mathbf{E}) = \epsilon_0 \chi^{(1)} \mathbf{E} + 0 + \epsilon_0 \chi^{(3)} \mathbf{E}\mathbf{E}\mathbf{E}$$

where \mathbf{E} is

$$\mathbf{E} = \frac{1}{2} (E_0 e^{ikz - i\omega t} + E_0^* e^{-ikz + i\omega t})$$

Put this eq. in (2.7), we get

$$\mathbf{P}(\mathbf{E}) = \epsilon_0 \left(\chi^{(1)} + \frac{3}{4} \chi^{(3)} |E_0|^2 \right) \mathbf{E}$$

Hence $\chi_{eff} = \chi^{(1)} + \frac{3}{4} \chi^{(3)} |E_0|^2$. We have relation between refractive index n and susceptibility χ_{eff}

$$n^2 = 1 + \chi_{eff} = 1 + \chi^{(1)} + \frac{3}{4} \chi^{(3)} |E_0|^2$$

$$n^2 = n_0^2 + \frac{3}{4} \chi^{(3)} |E_0|^2 = n_0^2 \left(1 + \frac{3 \chi^{(3)} |E_0|^2}{4 n_0^2} \right)$$

where we have used $n_0^2 = 1 + \chi_0$ (where n_0 is the linear component of refractive index). Now take square root on both sides and use binomial expansion; we get

$$n = n_0 \left(1 + \frac{3}{8 n_0^2} \chi^{(3)} |E_0|^2 \right) = n_0 + \frac{3}{8 n_0} \chi^{(3)} |E_0|^2$$

By using relation $I = \frac{1}{2}\epsilon_0 n_0 c |E_0|^2$

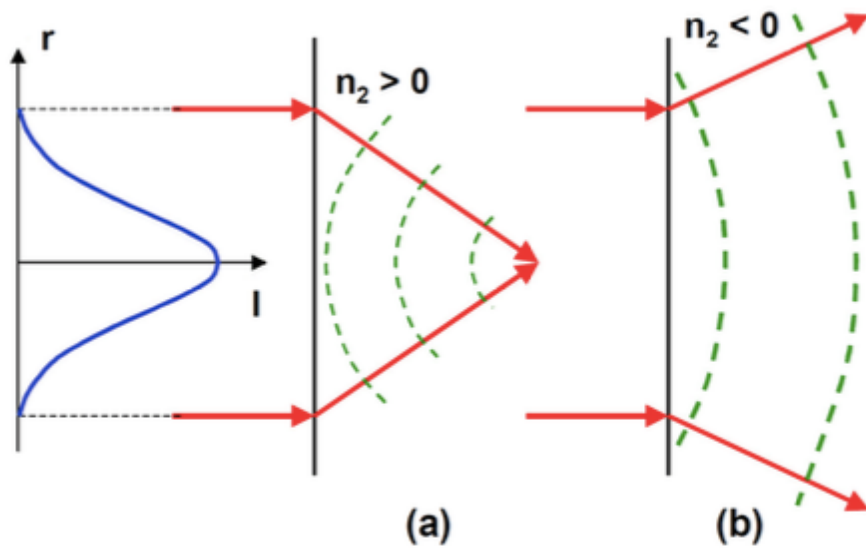
$$n = n_0 + \frac{3}{4}\chi^{(3)} \left(\frac{I}{\epsilon_0 n_0^2 c} \right)$$

$$n = n_0 + n_2 I$$

where $n_2 = \frac{3\chi^{(3)}}{4\epsilon_0 n_0^2 c}$ is a nonlinear component of the refractive index. And hence we can increase the nonlinear effects by increasing the intensity of incident light. This effect is known as the Optical Kerr effect, i.e., the change of refractive index of a material in response to an applied electric field.

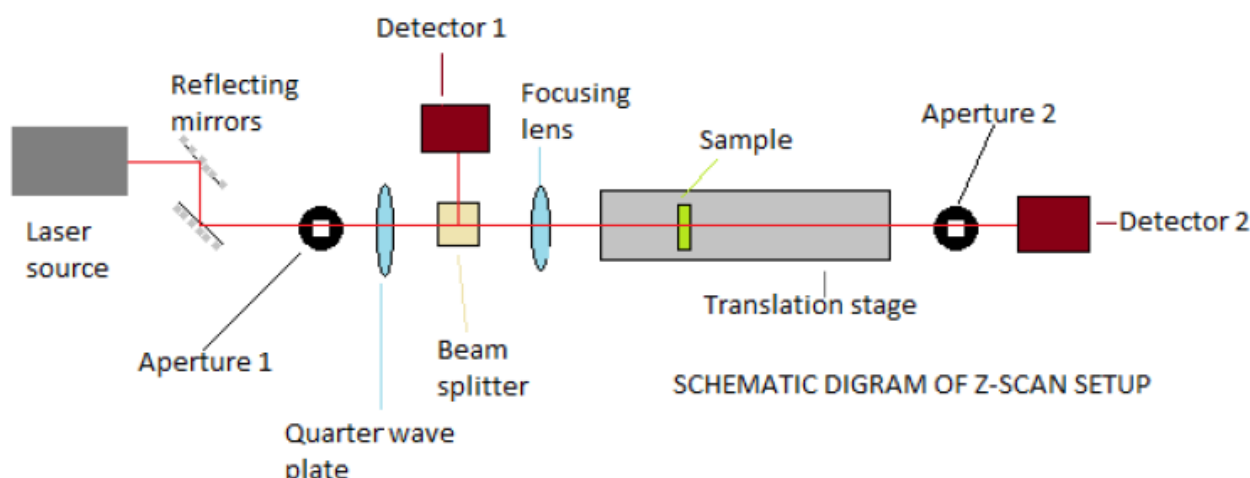
3.3.1 Self-focusing and defocusing

Self-focusing and defocusing is a non-linear optical process induced by the change in the refractive index of materials exposed to intense electromagnetic radiation. A medium whose refractive index increases with the electric field intensity acts as a focusing lens (fig a) for a Gaussian beam, while if it decreases with electric field intensity acts as a defocusing lens (fig b).

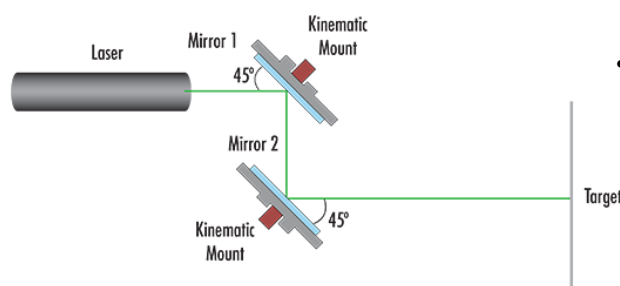


4 Z-Scan Experimental setup

4.1 Apparatus used and their Working



- Laser Source: We use the pulsed 532 nm laser.
- We used the two reflecting mirrors for aligning the beam by Parallel (Z-Fold) Configuration(as shown in below figure)



material. There are two types of beam-splitter. The first is the polarizing beam splitter(divides incident unpolarized light into orthogonally polarized beams), and the second is the Non-polarized beam splitter(split by a specific percentage independent of polarization).

- **Note:** We are using a combination of wave plate and beam-splitter to control the intensity of the laser beam. We will bring a polarisation in the light, and our beam splitter will split the beam intensity (will reflect some and pass some) as per polarisation.

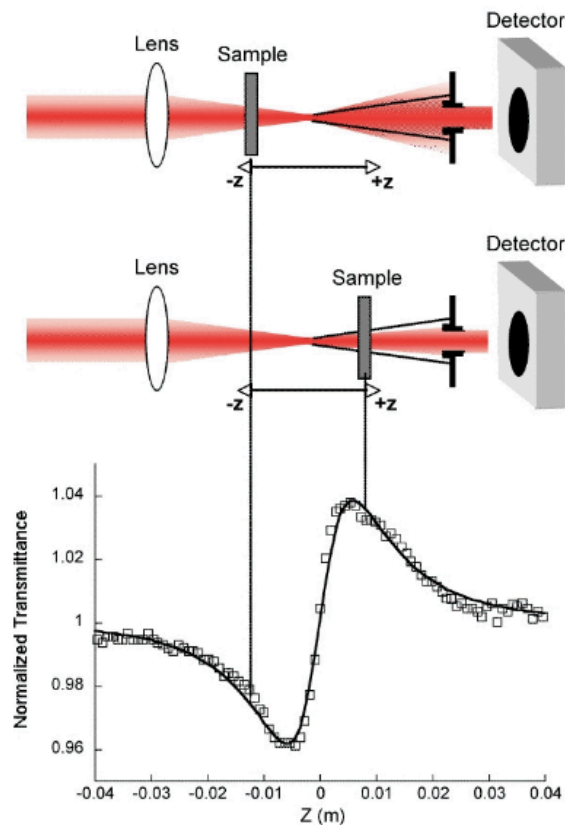
- Wave plate: Optical device which alters the polarization state of light-wave traveling through it. There are two types of wave plates, the first half wave plate, which shifts the polarization direction of linearly polarized light, second is a quarter-wave plate that converts linearly polarized light into circularly polarized light.
- Beam Splitter: Optical components are used to split incident light at a designated ratio into two separate beams. There will be semi-reflective the coating on one of the prism. The percentage of reflection/transmission depends on the coating
- Thermal detectors: It is based on the temperature change of the element through the absorption of EM radiation. A change in temperature causes a change in temperature-dependent property (resistance) of the thermal detector, which is evaluated electrically and measures the absorbed energy.
- A Converging Lens (L_0), with $f = 15$ cm, to focus on the LASER light.
- A Translation Stage (TS) with wires and control tools software. It has a stepper motor, running

at up to 300 RPM. The end-to-end length covered by the translation stage, with the mounted sample is 12.2 cm (~ 12400 steps).

- A Beam Profiler to measure the Beam Waist.
- An Optical Table to assemble the setup.
- Allen Keys and bolts to hold the equipment in place.
- Multiple screens to avoid interference from other setups.

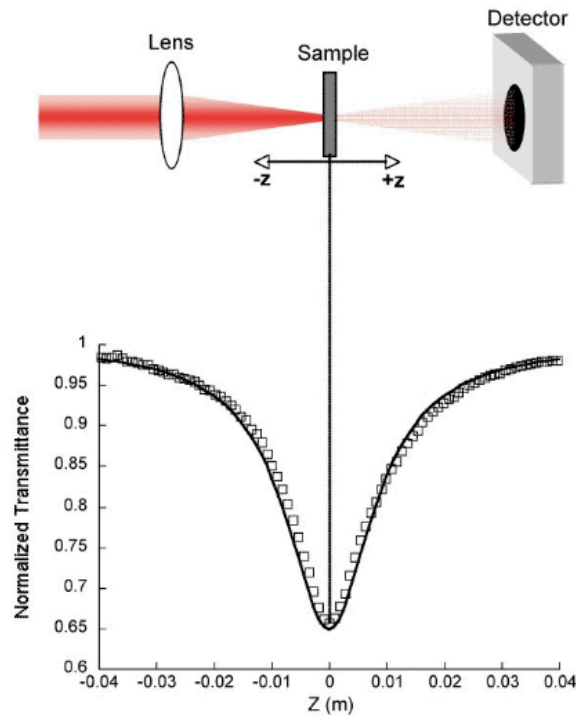
4.2 Principle

When a high-intensity laser beam propagates through a material, induced refractive index changes lead to the laser beam's self-focusing, which enables determining the third-order nonlinear optical properties of various materials. In this technique, the sample is translated in z-direction through the beam waist of a focused beam by keeping the input power of the beam constant. In our experiments, a continuous pulse wave laser operating at 532 nm, was used. The laser beam was focused using a 10 cm focal length lens. Let us consider a material with a positive non-linear refractive index, $n_2 > 0$. As shown in Fig. 1a), the non-linear lens shortens the beam's waist position to a negative z value on the side of focus where the beam is converging. As the beam passes through the shifted focus, it diverges at a greater diffraction angle, so the beam's power is spread over a wider area, and the beam passing through the pinhole decreases. When the sample is on the positive z side, where the beam is diverging, the non-linear lens reduces the beam's angle of divergence, thereby increasing the power passing through the pinhole. The effects are precisely opposite for $n_2 < 0$.



Refraction.png

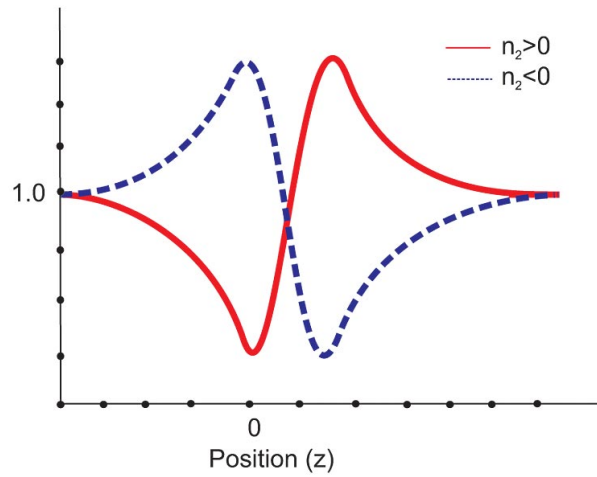
Non-Linear Refraction



Absorption.png

Non-Linear Absorption

If the material has a positive non linearity ($n_2 > 0$), the transmittance graph has a valley first and then a peak. For the sample with $n_2 < 0$ the graph is exactly the opposite (first peak and then valley).

Determination of a sign of n_2 from transmittance graph

The aperture plays an important role in determining which values we will find. We use a closed aperture to find out the non-linear refractive index and open aperture to find the absorption coefficient.

4.3 Formulas to derive Nonlinear refraction and nonlinear absorption

Consider a Gaussian Beam, propagating along the z -direction with beam waist, w_0 , wavelength, λ , and Rayleigh Length, $z_0 = \pi w_0^2 / \lambda$:

$$E(r, z) = E_0(t) \frac{w_0}{w(z)} \exp\left(-\frac{r^2}{w(z)^2}\right) \exp\left(-ikz - ik\frac{r^2}{2R(z)}\right) \exp(-i\phi(z, t)) \quad (1)$$

Here, $k = 2\pi/\lambda$ is the Wave Number; $w(z) = w_0(1 + x^2)$ represents the Beam Width, with $x = z/z_0$; and $R(z) = z(1 + x^2)$ denotes the Radius of Curvature. The last term, $\exp(-i\phi(z, t))$, contains all the radially uniform phase variations. As we only wish to obtain the radial phase variations, $\Delta\phi(r)$, we can apply the Slowly Varying Envelope Approximation (SVEA) and ignore phase uniform changes in r . Let this beam be transmitted through a Kerr non-linear optical material of length, L . Then, considering a centrosymmetric medium, we can write the refractive index and absorption coefficient as:

$$n(I) = n_0 + n_2 I, \quad (2)$$

$$\alpha(I) = \alpha_0 + \beta I \quad (3)$$

where, n_0 is the linear refractive index, while n_2 denotes the non-linear refractive index and α_0 is the linear absorption coefficient, while β represents the non-linear absorption coefficient. I denotes the intensity of light. For a thin sample, the output field can be written as follows:

$$E_{\text{out}} = E(r, z) e^{-\frac{\alpha_0 L}{2}} (1 + q)^{-\frac{ikn_2}{\beta} - \frac{1}{2}} \quad (4)$$

where, $q = \beta I L_{\text{eff}}$ with $L_{\text{eff}} = (1 - e^{-\alpha_0 L}) / \alpha_0$, and $I_0 = |E_0|^2$ is the on-axis intensity at beam waist. For very thin samples, such as in this experiment, we can take $L_{\text{eff}} \approx 1$ (in proper units). Moreover, I_0 can be written as:

$$I_0 = \frac{P_{\text{Avg}}}{RR \times PW \times (\pi w_0^2)}, \quad (5)$$

where, P_{Avg} is the average beam power, RR is the LASER Repetition Rate, PW is the LASER Pulse Width and πw_0^2 is the beam area, at focus.

The intensity distribution and phase shift of the beam at the exiting surface must also fulfill these criteria [2]:

$$I_{\text{out}}(r, z) = I(r, z) \frac{\exp(-\alpha_0 L)}{1 + q(r, z)} \quad (6)$$

and,

$$\Delta\phi = \frac{kn_2}{\beta} \ln(1 + q(r, z)) \quad (7)$$

Now, the intensity, $I(r, z)$, can be expressed as the product of I_0 and a local Gaussian profile, G_{local} [2], that can be written as follows:

$$G_{\text{local}} = \frac{1}{1 + x^2} \exp\left(-\frac{2r^2}{w^2(z)}\right) \quad (8)$$

When only NLR is present, we can write the non-linear phase change as:

$$\Delta\phi = \Delta\Phi_0 G_{\text{local}} \quad (9)$$

while for materials exhibiting pure NLA, q takes the following form:

$$q(r) = \Delta\Psi_0 G_{\text{local}} \quad (10)$$

Here, $\Delta\Phi_0$ and $\Delta\Psi_0$ are merely the results of the respective first order expansions of the expressions for $\Delta\phi$ (Eq. 7) and q , in the cases of pure NLR and pure NLA respectively. This gives us:

$$\Delta\Phi_0 = kn_2 I_0 L_{eff} \quad (11)$$

and,

$$\Delta\Psi_0 = 2^{-1.5} \beta I_0 L_{eff} \quad (12)$$

Substituting these quantities from Eq. 9 and Eq. 10 into Eq. 4, we obtain a final expression for the outgoing field:

$$E_{out} = E(r, z) e^{-\frac{\alpha_0 L}{2}} (1 + \Delta\Psi_0 G_{local})^{-\frac{i\Delta\Phi_0}{\Delta\psi_0} - \frac{1}{2}} \quad (13)$$

Now, making use of SVEA and the Gaussian Decomposition method for local field changes and considering only the first two terms in the decomposition, we can obtain an analytical expression for the complex, on-axis far-field given as ([1], [2]):

$$E_{out} = E(r, z) \exp\left(-\frac{\alpha_0 L}{2}\right) \sum_{n=0}^{\infty} \left[\frac{[-i\Delta\phi_0(z)]^n}{n!} \prod_{n'=0}^n \left(1 - i(2n' - 1) \frac{\Delta\Psi_0}{\Delta\Phi_0}\right) \right] \exp\left(\frac{-2nr^2}{w^2(z)}\right). \quad (14)$$

Using Eq. 14, we can write the complex field at the aperture planes as follows:

$$E_a = E(r, z) \sum_{n=0}^{\infty} \frac{[-i\Delta\phi_0(z)]^n}{n!} \prod_{n'=0}^n \left(1 - i(2n' - 1) \frac{\Delta\Psi_0}{\Delta\Phi_0}\right) \frac{w_{n0}}{w_n} \exp\left(-\frac{r^2}{w_n^2} - \frac{ikr^2}{2R_n} + i\theta_n\right) \quad (15)$$

Here, $\Delta\phi_0 = \Delta\Phi_0 / (1 + x^2)$

When only NLR is considered, $\Delta\Psi_0 \rightarrow 0$, and we can reduce the previous equation to obtain:

$$E_a = E(r, z) \sum_{n=0}^{\infty} \frac{[-i\Delta\phi_0(z)]^n}{n!} \frac{w_{n0}}{w_n} \exp\left(-\frac{r^2}{w_n^2} - \frac{ikr^2}{2R_n} + i\theta_n\right) \quad (16)$$

Taking d to be the propagation distance in free space between the sample and the aperture and $g = 1 + d/R(z)$, we can represent the parameters in Eq. 15 and 16 as follows:

$$w_{n0}^2 = \frac{w^2(z)}{2n + 1}$$

$$d_n = \frac{kw_{n0}^2}{2}$$

$$w_n^2 = w_{n0}^2 \left(g^2 + \frac{d^2}{d_n^2}\right)$$

$$R_n^2 = d \left(1 - \frac{g}{g^2 + d^2/d_n^2}\right)^{-1}$$

and,

$$\theta_n = \tan^{-1} \left(\frac{d}{gd_n} \right)$$

The total transmitted power through the aperture can then be obtained by spatially integrating $E_a(r, t)$, like so:

$$P_T(\Delta\Phi_0(t)) = \int_0^{r_a} |E_a(r, t)|^2 r \, dr \quad (17)$$

This directly yields the normalized Z-scan transmittance, $T(z)$, using the following expression:

$$T(z) = \frac{\int_{-\infty}^{\infty} P_T(\Delta\Phi_0(t)) \, dt}{S \int_{-\infty}^{\infty} P_i(t) \, dt} \quad (18)$$

where $P_i(t) = \pi w_0^2 I_0(t)/2$ is the instantaneous input power, within the sample, and $S = 1 - \exp(-2r_a^2/w_a^2)$, where subscript - a denotes "aperture". This is where the aperture-dependence of the Z-Scan traces comes in. For closed aperture traces, we can take $S \approx 0$ and for open aperture traces, $S \approx 1$. Now, the normalized transmittance for the on-axis electric field, at the aperture plane, can be written as:

$$T_2(z, \Delta\phi_0) = \frac{|E(r=0, z, \Delta\phi_0)|^2}{|E(r=0, z, \Delta\phi_0=0)|^2} \quad (19)$$

On substituting the expression for the field into Eq. 19 and simplifying, we obtain the final expression for $T(z)$, that considers the effect of both NLR and NLA, as given below:

$$T_2(z, \Delta\Phi_0, \Delta\Psi_0) = 1 + \frac{4\Delta\Phi_0 x}{(x^2 + 9)(x^2 + 1)} - \frac{\Delta\Psi_0}{x^2 + 1} \quad (20)$$

Eq. 20 provides a two-parameter fitting function for any third-order Z-Scan trace, the two parameters being $\Delta\Phi_0$ and $\Delta\Psi_0$. We have used it to fit the closed aperture traces to obtain the n_2 values in this experiment. On the other hand, for β values, we take the open aperture traces that de-emphasize $\Delta\Phi_0$ or minor intensity variations as the entire signal is being measured. So, we can provide a more straightforward, one-parameter expression for $T(z)$ in this case:

$$T_2(z, \Delta\Phi_0=0, \Delta\Psi_0) = 1 - \frac{\Delta\Psi_0}{x^2 + 1} \quad (21)$$

Equations 20 and 21 are the working formulae for this experiment. Figure 4 shows variations in transmittance in Z-scan traces for materials exhibiting pure NLR, pure NLA, and both NLR and NLA (mixed case), using various values for $\Delta\Phi_0$ and $\Delta\Psi_0$. It is clear from the plots that NLA suppresses peaks in the mixed Z-Scan traces compared to the pure NLR case. This also means that the symmetric nature of pure NLR curves is usually absent in most Z-Scan traces, where both NLR and NLA contribute. As such, we can utilize another

interesting quantity, which is the Peak-Valley Transmittance Change, ΔT_{p-v} . It is expressed as follows in the closed aperture case (where we shall be using the two-parameter fitting function in Eq. 20):

$$\Delta T_{p-v} = 0.406 \Delta \Phi_0 \quad (22)$$

This relation for ΔT_{p-v} should hold even for highly skewed Z-Scan traces. Therefore, it provides us with an excellent tool to verify the quality of our traces.

5 Z-Scan Experiment

5.1 Toluene

Specification of the Experimental setup.

- Effective length of the sample, $L_{eff} = 1 \text{ mm}$
- Repetition rate of Laser = 80kHz
- Pulse width at a given repetition rate = 1.75 ns
- Beam waist of a laser beam = $35 \times 10^{-6} \text{ m}$

5.1.1 Observation And Results

Open Aperture

- RPM of motor = 300
- PowerAverage = 82.07mW
- Non-linear absorption coefficient, $\beta = (1.307 \pm 0.0814) \times 10^{-8} \text{ mW}^{-1}$

Close Aperture

- RPM of motor = 300
- PowerAverage = 23.11mW
- Non-linear refractive index, $n_2 = -(2.711 \pm 0.0941) \times 10^{-15} \text{ m}^2 \text{W}^{-1}$

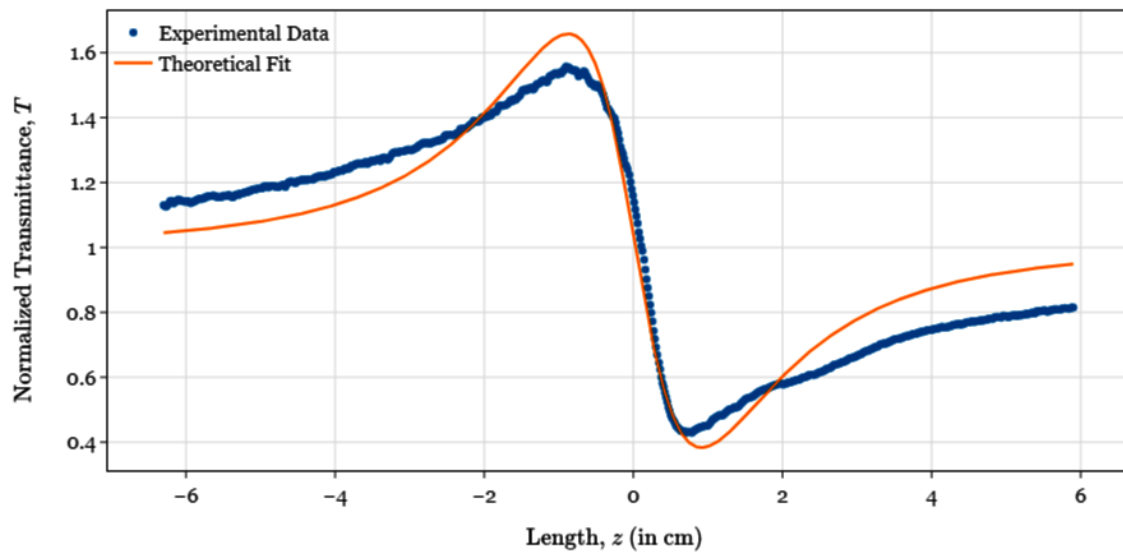


Figure 1: Closed aperture

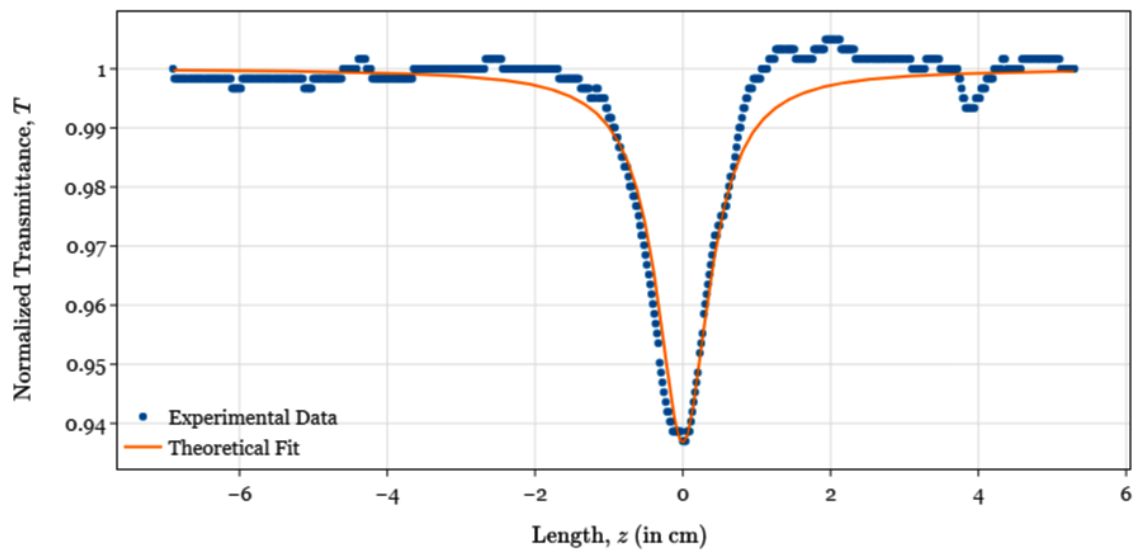


Figure 2: Open aperture

5.2 Acetone

Specification of the Experimental setup.

- Effective length of the sample, $L_{eff} = 1$ mm
- Repetition rate of Laser = 80kHz
- Pulse width at a given repetition rate = 1.75 ns
- Beam waist of a laser beam = 35×10^{-6} m

5.2.1 Observation And Results

Open Aperture

- RPM of motor = 300
- Average power = 185.7mW
- Non-linear absorption coefficient, $\beta = (1.052 \pm 0.0432) \times 10^{-8} \text{ mW}^{-1}$

Close Aperture

- RPM of motor = 300
- Average power = 24.22mW
- Non-linear refractive index, $n_2 = -(2.752 \pm 0.6822) \times 10^{-14} \text{ m}^2 \text{W}^{-1}$

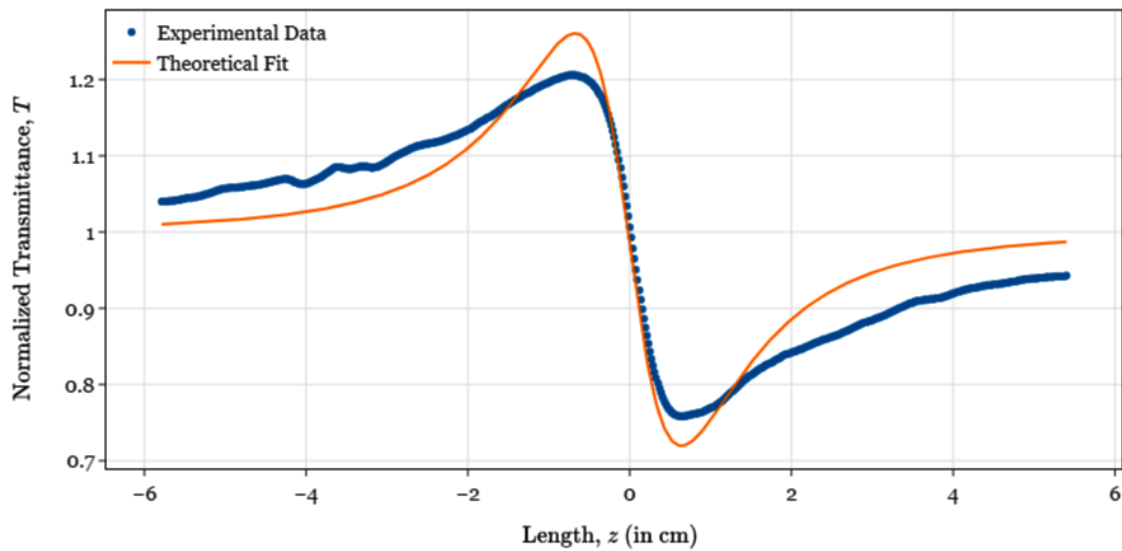


Figure 3: Closed aperture

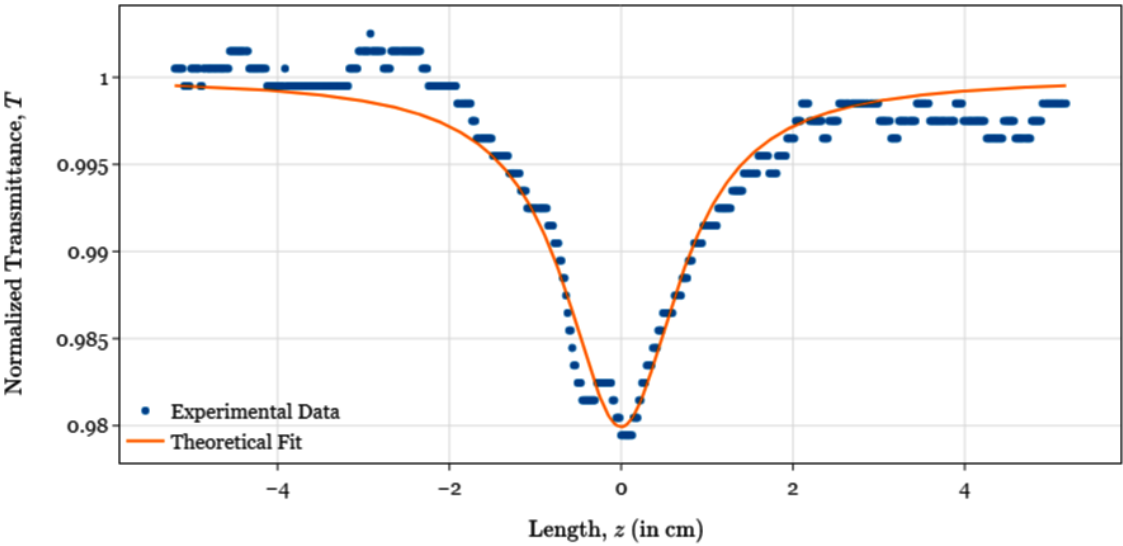


Figure 4: Open aperture

6 Conclusion

We can use the Z-scan experimental configuration to obtain the nonlinear refractive index and nonlinear absorption coefficients of any standard samples. The sign and magnitude of the nonlinear refractive index of the samples can be measured. We will then use the equations of normalized transmittance and fit them with the data points and report the refractive index and nonlinear absorption coefficients. The property of a nonlinear sample to change refractive index on changing intensity can be used to make an optical transistor type of thing.

7 Improvement and New ideas on the Setup

We want to make an optical transistor. In other words, we want to control the intensity of one laser by changing the intensity of another laser. To get it, we planned to use the nonlinear property of the material. So we made different setups to achieve our goals.

We plan to combine Z scan and Michaelson Morley setup in our first setup. To see whether it is possible to see the change in the refractive index through another laser beam.

7.1 Setup 1 and Explanation

We plan to combine Z scan and Michaelson Morley (MM) setup in our first setup. Here, we made the laser from one arm of the MM Setup pass through the same place of the sample where the laser from the Z Scan arm was already hitting. By changing the intensity of the Z-scan arm, we can change the refractive index of the medium(Sample), and since one arm of the MM Setup laser is also falling at the same place of the sample, it will also face some path length change. Our goal was here to see the change in the fringe pattern of the interferometer by changing the intensity of the Z Scan arm laser. Before we could complete the setup and alignment of our first setup, we saw something interesting, which made us go for Setup-2.

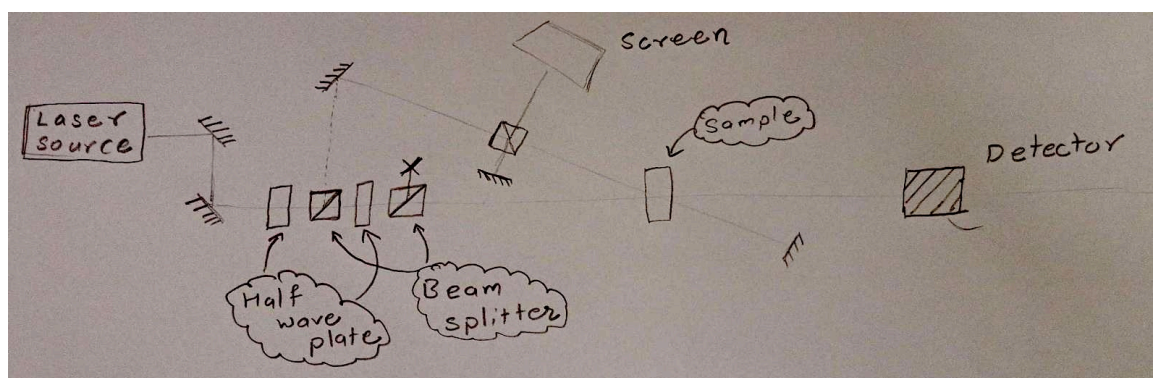


Figure 5: Setup-1

7.2 Setup 2 and Explanation

When we were doing Setup 1, we observed a black spot in the MM setup's arm falling on the Screen (marked in Setup 2). From now we will call the arm of MM as **Probe Beam** and the Z-scan arm as **Push beam**. Here our push beam is focused, and the probe beam is not.

In explaining this black dot formation, we believe that our push beam, which is focused, is forming a strong lens in the Centre of the sample. Here we are keeping the intensity of our push beam higher than the intensity

of the probe beam. Now when our unfocused low-intensity probe beam falls on the sample (where a strong lens kind of thing is formed due to push beam), then some part of the probe beam which is directly falling on the lens we call it **Inner probe beam** and the rest is called the **outer probe beam**. Light of inner probe beam hits that area of the sample, where lens effect is strong, the inner beam gets conversed and diverse as we move further away from focus in the direction of the probe beam. So the intensity of the inner beam will spread to a large area. But the area on the screen where the inner beam would have hit when there was no sample has light coming from only the inner beam and when the sample is there. Since it is defocused, the light intensity is very low in the central area.

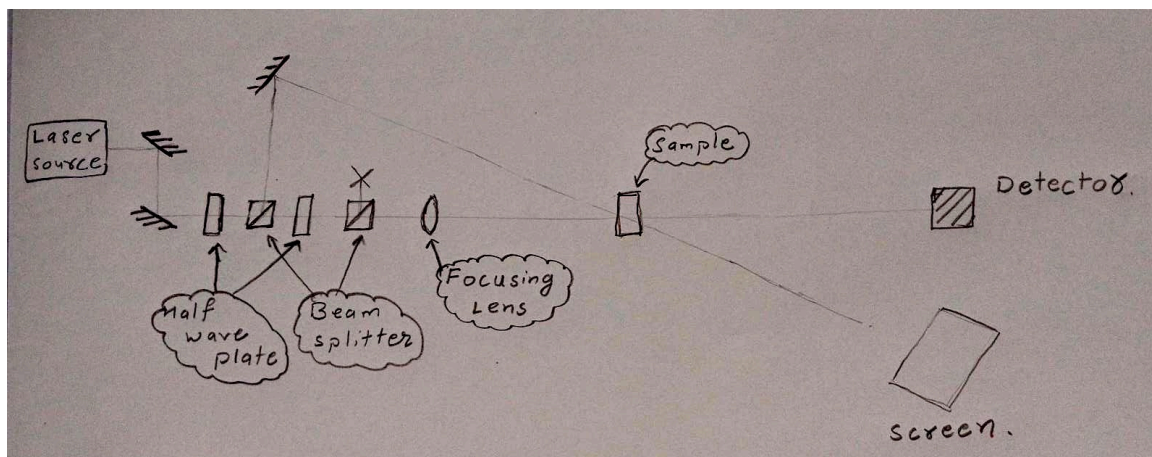


Figure 6: Setup-2

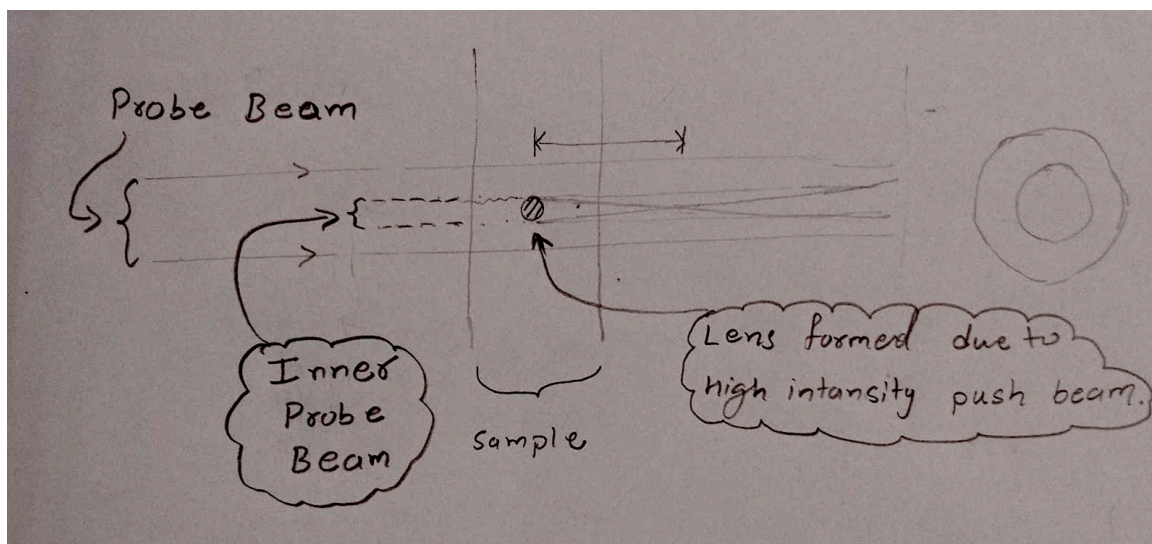


Figure 7: Focusing of Inner probe beam

The exciting thing about this black spot is that it disappears when we stop the push beam from passing through the sample. This allows us to build the optical transistor using these phenomena.

So for making an optical transistor, we first blocked the light using an aperture so that only the black dot area has some intensity on the screen and only gets the light of the probe beam, which is changing while changing the intensity of the push beam. We want our optical transistor to pass higher information from push

beam to probe beam.

When we were varying the push beam intensity from 0 to 156mW, we were getting the blocked probe beam intensity to be changing from 38mW to 2mW. This difference is significant to be measured. To make the difference more visible, we planned to create a new setup.

7.3 Setup 3 and Explanation

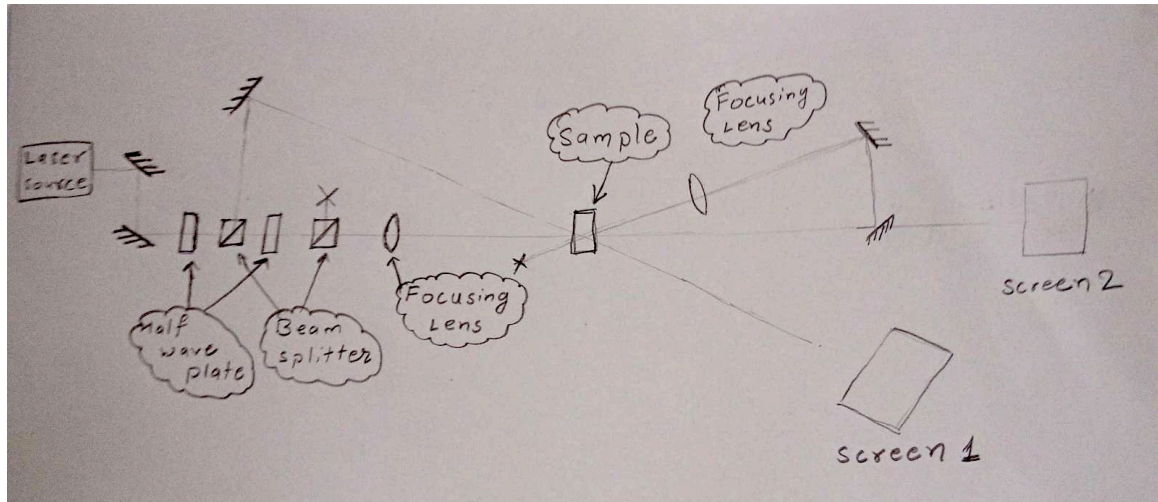


Figure 8: Setup-3

So in this setup, we made our push beam fall on our sample twice using mirror arrangements and got some significant improvements. When we varied the push beam intensity from 0 to 156 mW, we saw a change in our probe beam intensity from 55 to 2 mW.

7.4 Setup 4 and Explanation

Our sample has a positive n_2 value, so the light passing through the sample will move toward higher intensity. We used this to make the black hole bigger and converge the Gaussian beam to have more intensity in the center. Then we used the two aperture to increase the effect of intensity difference. When we were varying the intensity of our push beam from 0 to 80mW, we observed a change in our probe beam intensity from 67mW to 3mW, which is better than all the previous setups.

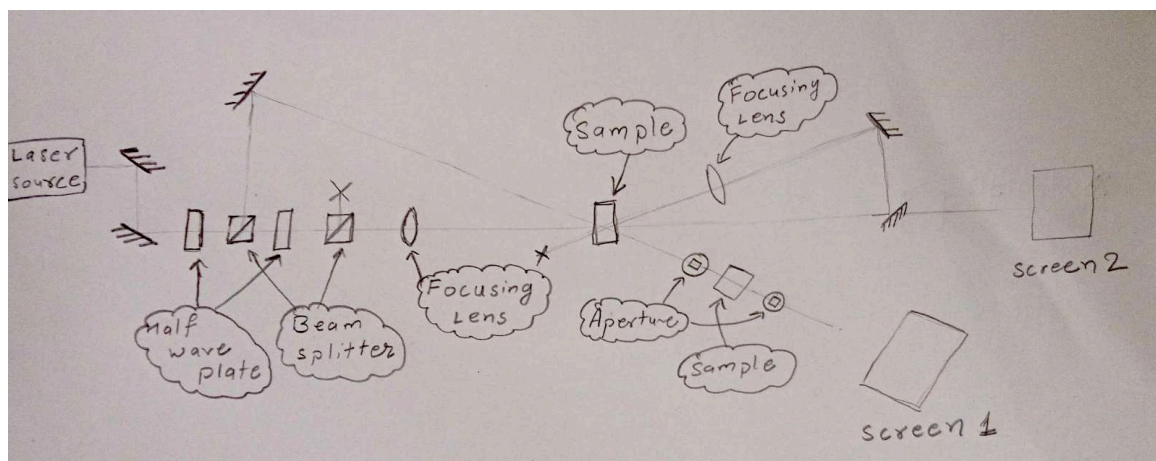


Figure 9: Setup-4

8 Photos and Results

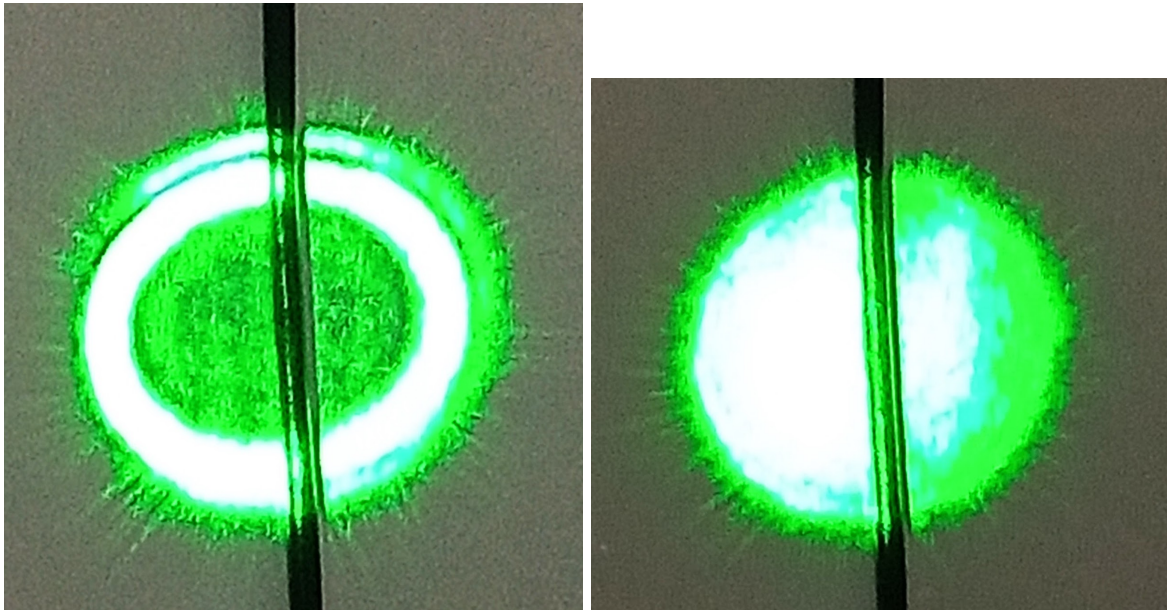


Figure 10: With Push beam on and then Stopped in Setup-3

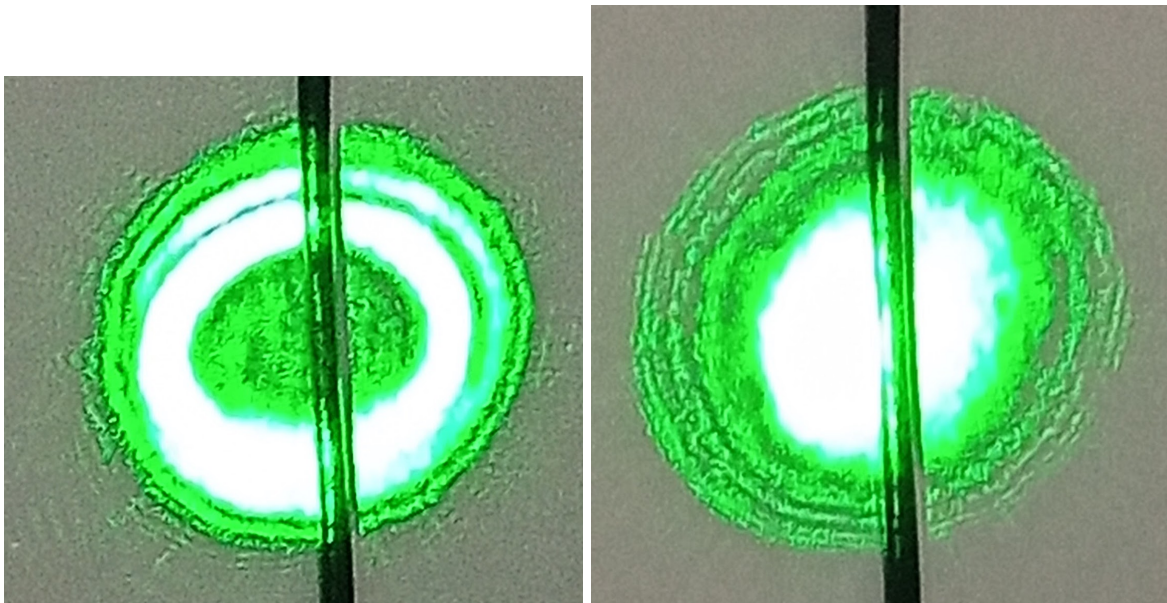


Figure 11: With Push beam on and then Stopped in Setup-4

In Figure 10 from setup- 3, here we do not have that extra sample. we are getting a black spot in the probe beam when the push beam is on, and when we stop the push beam, the black spot is filled with a bright light. In Figure 11 from setup-4, here we have that extra sample. When the push beam is on, we get the dark black spot in the probe light; this time, the dark area is more darker and smaller. When we stop the push beam and see the probe beam, then in place of the dark spot, we get a more brighter light in comparison with Figure 3. This shows that setup-4 is better and is really an improvement of setup-3 to make a better optical transistor.

9 Advantages and Disadvantages of Z-Scan

Advantages

- It is a simple and susceptible technique to measure the sign and magnitude of nonlinear refraction and absorption coefficients.
- It has no difficult alignment other than beam aligning on the aperture.
- Data analysis is quick and simple.
- It can determine both real and imaginary parts of $\chi^{(3)}$.
- Z-scan can also be modified to study non-linearities of higher-order contributions.

Disadvantages

- It requires a high-quality Gaussian TEM_{00} beam for absolute measurements.
- The analysis must be different if the beam is non-Gaussian.
- Sample distortions, tilting of the sample during translation, can cause the beam to walk off the far-field aperture.

10 Precautions and Sources of Error

- The polariser should be used to reduce the power of the laser to reduce the thermal effects of the laser on the samples.
- Protective glasses must be worn while taking measurements, and the laser beam shouldn't be allowed to fall outside here, thereby carefully blocking it with a black aluminum plate.
- The lasers should be turned off when not in use.

11 References

- M. Sheik-Bahai, A. A. Said, T. H. Wei, D. J. Hagan, and E. W. van Stryland, Sensitive measurement of optical nonlinearities using a single beam, IEEE Journal of Quantum Electronics 26, 760 (1990).
- A. B. Ortega, M. L. A. Carrasco, M. M. M. Otero, E. R. Lara, E. V. G. Ramírez, and M. D. I. Castillo, Analytical expressions for z-scan with arbitrary phase change in thin nonlocal nonlinear media, Opt. Express 22, 27932 (2014).
- A. E. Siegman, How to (maybe) measure laser beam quality, in DPSS (Diode Pumped Solid State) Lasers: Applications and Issues (Optical Society of America, 1998) p. MQ1.
- L. T. Nguyen, N. T. Hong, C. T. B. Thi, and A. Q. Le, The numerical methods for analyzing the Z-scan data, Journal of Nonlinear Optical Physics and Materials 23, 1450020 (2014).

- R. Rangel-Rojo, S. Yamada, H. Matsuda, H. Kasai, H. Nakanishi, A. K. Kar, and B. S. Wherrett, Spectrally resolved third-order nonlinearities in polydiacetylene microcrystals: influence of particle size, J. Opt. Soc. Am. B 15, 2937 (1998).
- M. Yüksek, A. Elmali, M. Karabulut, and G. M. Mamedov, Switching from negative to positive nonlinear absorption in p-type 0.5 atcrystal, Optical Materials 31, 1663 (2009).